

Three-Dimensional Magnetic Resonance Imaging Quantification of Glenoid Bone Loss Is Equivalent to 3-Dimensional Computed Tomography Quantification: Cadaveric Study

Adam B. Yanke, M.D., Jason J. Shin, M.D., Ian Pearson, B.S., Bernard R. Bach Jr., M.D., Anthony A. Romeo, M.D., Brian J. Cole, M.D., M.B.A., and Nikhil N. Verma, M.D.

Purpose: To assess the ability of 3-dimensional (3D) magnetic resonance imaging (MRI, 1.5 and 3 tesla [T]) to quantify glenoid bone loss in a cadaveric model compared with the current gold standard, 3D computed tomography (CT). **Methods:** Six cadaveric shoulders were used to create a bone loss model, leaving the surrounding soft tissues intact. The anteroposterior (AP) dimension of the glenoid was measured at the glenoid equator and after soft tissue layer closure the specimen underwent scanning (CT, 1.5-T MRI, and 3-T MRI) with the following methods (0%, 10%, and 25% defect by area). Raw axial data from the scans were segmented using manual mask manipulation for bone and reconstructed using Mimics software to obtain a 3D en face glenoid view. Using calibrated Digital Imaging and Communications in Medicine images, the diameter of the glenoid at the equator and the area of the glenoid defect was measured on all imaging modalities. **Results:** In specimens with 10% or 25% defects, no difference was detected between imaging modalities when comparing the measured defect size (10% defect $P = .27$, 25% defect $P = .73$). All 3 modalities demonstrated a strong correlation with the actual defect size (CT, $\rho = .97$; 1.5-T MRI, $\rho = .93$; 3-T MRI, $\rho = .92$, $P < .0001$). When looking at the absolute difference between the actual and measured defect area, no significance was noted between imaging modalities (10% defect $P = .34$, 25% defect $P = .47$). The error of 3-T 3D MRI increased with increasing defect size ($P = .02$). **Conclusions:** Both 1.5- and 3-T-based 3D MRI reconstructions of glenoid bone loss correlate with measurements from 3D CT scan data and actual defect size in a cadaveric model. Regardless of imaging modality, the error in bone loss measurement tends to increase with increased defect size. Use of 3D MRI in the setting of shoulder instability could obviate the need for CT scans. **Clinical Relevance:** The goal of our work was to develop a reproducible method of determining glenoid bone loss from 3D MRI data and hence eliminate the need for CT scans in this setting. This will lead to decreased cost of care as well as decreased radiation exposure to patients. The long-term goal is a fully automated system that is as approachable for clinicians as current 3D CT technology.

From the Sports Medicine Division, Department of Orthopaedics, Rush University (A.B.Y., B.R.B., A.A.R., B.J.C., N.N.V.), Chicago, Illinois, U.S.A.; Department of Orthopaedics, Royal University Hospital, University of Saskatchewan (J.J.S.), Saskatoon, Canada; and Rush University Medical School (I.P.), Chicago, Illinois, U.S.A.

The authors report the following potential conflicts of interest or sources of funding: A.B.Y. receives support from the Arthroscopy Association of North America (research grant paid to institution), and NuTech and Arthrex (research support). J.J.S. receives support from the Arthroscopy Association of North America (research grant paid to institution). I.P. receives support from the Arthroscopy Association of North America (research grant paid to institution). B.R.B. receives support from the Arthroscopy Association of North America (research grant paid to institution), American Orthopaedic Society for Sports Medicine (board membership fees), Slack (royalties), and research support from Arthrex, Commed Linvatec, DJ Orthopaedics, Ossur, Smith & Nephew, and Tornier. A.A.R. receives support from the Arthroscopy Association of North America (research grant paid to institution); American Orthopaedic Society for Sports Medicine, American Shoulder and Elbow Surgeons, and Arthroscopy Association of North America (board membership fees); Arthrex (consultancy fees, grants/grants pending, royalties, payment for development of educational presentations); and DJO Surgical, Smith & Nephew, and Ossur

(grants/grants pending). B.J.C. receives support from the Arthroscopy Association of North America (research grant paid to institution); Arthrex, DJ Orthopaedics, Johnson & Johnson, Regentis, and Zimmer (consultancy fees); Johnson & Johnson, Medipost, Zimmer Comments (research support); Arthrex, DJ Orthopaedics, Elsevier, Lippincott, Smith & Nephew, WB Saunders (royalties); and Carticapt, Regentis (stock/stock options). N.N.V. receives support from the Arthroscopy Association of North America (research grant paid to institution); Smith & Nephew (board membership fees); Smith & Nephew, MinInvasive (consultancy fees); Smith & Nephew (payment for lectures including service on speakers bureaus); Smith & Nephew, and Vindico Medical-Orthopedics Hyperguide (royalties).

The Arthroscopy Association of North America provided support for this study with a research grant.

Received May 3, 2015; accepted August 25, 2016.

Address correspondence to Adam B. Yanke, M.D., Rush University Medical Center, 1611 W Harrison St., Suite 300, Chicago, IL 60614, U.S.A. E-mail: Adam.Yanke@RushOrtho.com

© 2016 by the Arthroscopy Association of North America
0749-8063/15371/\$36.00

<http://dx.doi.org/10.1016/j.arthro.2016.08.025>

In young athletes who participate in high-risk sports, recurrent anterior shoulder instability is common following an initial traumatic dislocation.¹ Glenoid bone loss has been reported in up to 73% of recurrent dislocators.² Critical-sized glenoid defects are associated with a recurrence rate of 67% to 89% after soft tissue stabilization alone.³⁻⁵ Yamamoto et al.⁶ showed in a cadaveric study that osseous defects $\geq 19\%$ of the glenoid width are unstable even after Bankart repair. Therefore, during presurgical planning for shoulder stabilization, recognizing and accurately quantifying the amount of glenoid bone loss is critical.

Clinical determination of glenoid bone loss can be performed via plain radiographs, computed tomography (CT), or magnetic resonance imaging (MRI). Although radiographs are useful in screening for glenoid bone loss, based on cadaveric studies, the prediction error and standard deviation of plain radiographs are double those of CT or MRI.⁷ Radiographs and even 2-dimensional (2D) advanced imaging modalities, such as MRI or CT, are less accurate because of sensitivity to patient positioning and scanning technique. Although 2D MRI is similar to 2D CT in determining bone loss,⁸ cadaveric and clinical studies have shown that both are clearly inferior to 3-dimensional (3D) CT.^{7,9}

Three-dimensional CT allows for simplified patient positioning and, with reformatting, the humeral head can be subtracted to provide an unobstructed view of the glenoid. Therefore, 3D CT has been found to be accurate and reliable in representing the complex glenoid anatomy, and thus emerged as the gold standard.^{7,9-11} CT scans also carry the added risk of exposing the patient to 2.06 mSv of irradiation.¹² This is roughly equivalent to the amount of background radiation (ubiquitous ionizing radiation, including natural and artificial sources, that individuals on Earth are exposed to) one is exposed to over 8 months, which can be significant for young adults.¹³

Currently, MRI is the reference standard when assessing soft tissue and is typically ordered by clinicians prior to obtaining a CT scan to evaluate the surrounding non-osseous structures after shoulder dislocation.¹⁴⁻¹⁶ The ability to use a single study to evaluate both soft tissue injury and bone loss would establish MRI as the preferred imaging modality for evaluating instability pathology. Previous reports have demonstrated conflicting outcomes when comparing CT to MRI for quantification of glenoid bone loss and most have used suboptimal cadaveric models with bone only after soft tissue dissection.^{7,8,17,18}

The purpose of this study was to assess the ability of 3D MRI (1.5- and 3-tesla [T]) to quantify glenoid bone loss in a cadaveric model compared with the current gold standard, 3D CT. Our hypothesis was that both

1.5- and 3-T 3D MRI would have similar measurement error as 3D CT.

Methods

We received investigational review board exempt status for this cadaveric study. Six whole fresh-frozen shoulders (6 males, 3 right, 3 left, age range: 63-72 years old) were used for the study. None of the specimens had a history of shoulder trauma or previous shoulder surgery. All specimens were inspected to confirm intact labrum, bone, and articular surfaces. The specimens were frozen at -20°C and thawed overnight at room temperature on the day of testing for a single freeze-thaw cycle.

Before imaging, the shoulders underwent an extended deltopectoral approach to expose the glenohumeral joint. This exposure included soft tissue take-down of the subscapularis to allow for later repair. After dissection, the labrum was elevated and mobilized using an arthroscopic elevator. The anteroposterior (AP) dimension of the glenoid was measured by the operating surgeon through the bare area with a handheld digital caliper (0.1 mm resolution) in a manner similar to that used clinically with an arthroscopic probe. A gross photograph (Canon PowerShot S100) was recorded using a paper ruler for calibration. The shoulder was then subsequently closed in layers using nonabsorbable braided suture. Specifically, the subscapularis was closed with no. 2 Ethibond suture, repairing the tendon to the remaining tendon that remained on the lesser tuberosity. Care was taken to keep the labrum intact, although a formal repair was not performed with regard to the labrum. The specimen then underwent scanning (CT, 1.5-T MRI, and 3-T MRI) without defect creation.

Both 1.5- and 3-T MRI scans used T1 coronal, sagittal oblique, and axial views. T1 weighting was selected because it most accurately represents osseous detail.¹⁹ The 1.5-T MRI (Magnetom Essenza; Siemens Healthcare) protocol included the following: slice thickness 3.5 mm, gap 1.0 mm, response time 479 milliseconds, echo time 16 milliseconds, and field of view 160 mm. The 3-T MRI (Magnetom Verio; Siemens Healthcare) protocol included the following: slice thickness 2.0 mm, gap 0.5 mm, response time 400 milliseconds, echo time 22 milliseconds, and field of view 130 mm. The CT scans, which were obtained in coronal, sagittal oblique, and axial planes by use of 0.625 mm contiguous slices (120 kV, 260 mA) (Fig 1), were then processed into 3D en face glenoid (sagittal oblique) views with humeral subtraction (Volume Viewer 8.9.21; GE Healthcare).

Dissection was carried out again to create glenoid defects correlating to 10% glenoid bone loss. Using

trigonometry, the previously measured intact glenoid diameter (D) was used to determine the amount of glenoid resection needed to correspond to 10% loss by area. This was calculated by measuring the maximum AP distance of the glenoid using a digital caliper. The equation from Bhatia et al.²⁰ was rearranged, and the diameter was then used to calculate how much of a decrease in diameter (w) was necessary to create the given percentage of bone loss based on circle area (Fig 2).

$$\text{Percent bone loss} = \left(\frac{1}{2\pi} \right) \left(2 * \arccos \left(1 - 2 \left(\frac{w}{D} \right) \pi \right) - \sin \left(2 * \arccos \left(1 - 2 \left(\frac{w}{D} \right) \pi \right) \right) \right) * 100\%$$

Using a combination of a Dremel rotary tool (Robert Bosch Tool, Mount Prospect, IL) and rasps, anatomic anterior glenoid bone defects parallel to the plane of the scapula and long axis of glenoid were created.²¹ The anterior-based defects were created as a chord perpendicular to the AP diameter of the glenoid circle estimation. After defect creation, the AP dimension of the defected glenoid was measured, a photograph with calibration rule placed was recorded, and the soft tissues were repaired as described and reimaged. This protocol was repeated for 25% glenoid area defect. After each sequential defect, repeat imaging was carried out.

For MRI 3D reformatting, raw axial data from the 1.5-T MRI (T1) and 3-T MRI (gradient T1) scans were segmented using manual mask manipulation for bone and reconstructed into 3D files using Mimics 13.1 software (Materialise, Leuven, Belgium). Calibrated Digital Imaging and Communications in Medicine images of 3D en face glenoid views were created for all imaging modalities. The images were presented in a randomized order to 3 sports medicine fellowship-trained orthopedic surgeons blinded to the true anatomic measurements, as well as the study design, who determined the percentage area bone loss using the Pico method described by Baudi et al.²² This method was chosen as the inferior portion of the glenoid can accurately be represented by a circle.²³ Using the area of the circle (surface A) and the area of the defect (surface B), the percentage of bone loss was calculated (surface B/surface A \times 100) as described by Sugaya et al.²⁴ (OsiriX, Pixmeo SARL, 2003-2014).

Each shoulder underwent 3 rounds of imaging after glenoid preparation (0%, 10%, and 25% osseous defect) using 3 imaging modalities (CT, MRI 1.5-T, and MRI 3-T) and yielded a series of 9 models per shoulder. Six shoulders were analyzed, resulting in a total of 54 models subject to imaging quantification, which were then compared with 15 manually measured anatomic values. A master key with the exact measurements of bone loss were kept by one of the study authors (J.J.S.).

Power analysis was based on pilot data using defect surface area percentage as the primary outcome. Assuming a 3% difference between groups and a standard deviation of 2.5%, 6 samples were needed to obtain a power of 80%. The error of the imaging modality was calculated based on the absolute difference between the actual defect size and the measured defect size. These 3 measurements were compared using analysis of variance (ANOVA with post hoc Tukey test). Pearson correlation coefficients (ρ) were calculated between the different modes of measurement with regard to calculated defect area and absolute difference in measured defect area. Significance for all tests was set at $P < .05$. Statistical calculations were carried out using the XLSTAT suite in Microsoft Excel (Microsoft, Redmond, WA).

Results

With regard to the intact samples, no specimens were measured as having a defect when none were present. In specimens with 10% or 25% defect, no difference was detected between imaging modalities when comparing the measured defect size (ANOVA 10% defect: 0.27, ANOVA 25% defect: 0.73) (Table 1). All 3 modalities demonstrated a strong correlation with the actual defect size (CT, $\rho = .97$; 1.5-T MRI, $\rho = .93$; 3-T MRI, $\rho = .92$, $P < .0001$). Similarly, there was a significant correlation when comparing imaging modalities with each other ($P < .0001$) (Table 2, Fig 3). When looking at the absolute difference between the actual and measured defect area, no significance was noted between imaging modalities (ANOVA, 10% defect: 0.34; ANOVA, 25% defect: 0.47) (Table 3). The error of 3-T MRI increased significantly with increasing defect size ($P = .022$). Although not statistically significant, the difference in error for 3D CT measurements approached significance ($P = .07$). When looking at all samples—measured defect size plotted against actual defect size—all 3 study modalities either over- or underestimated the defect size in the 10% defect group, in 5 of 6 samples (Fig 4). A similar pattern was noticed in the 25% defect size.

Discussion

The principal finding of this investigation is that in a cadaveric model with controlled defect size, there is no difference in the measurement of 10% and 25% area glenoid defects between CT, 1.5-T MRI, and 3-T MRI. This is the first study to compare all 3 modalities with anatomic measurements as the gold standard. Moreover, the results of this investigation demonstrate several points with regard to the use of 3D MRI for measuring glenoid bone loss.

The specific methodology used in studies evaluating the accuracy of glenoid bone loss measurements based

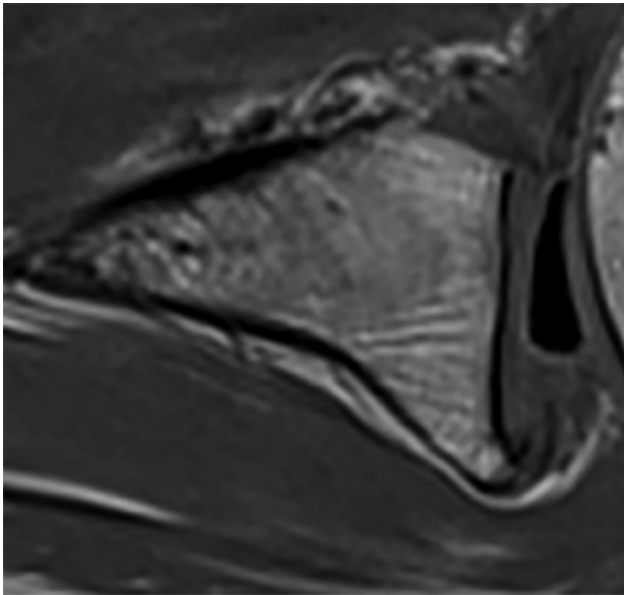


Fig 1. Representative axial T1 sequence in a cadaver with a 10% defect.

on imaging modalities can have a significant effect on the study results. Specifically, all studies that remove the soft tissue surrounding the glenoid create an artificial glenoid-air border interface as opposed to the natural glenoid-labral junction. Because of the similar intensities of glenoid cortex and glenoid labral signal on MRI, the presence of the labrum is important in

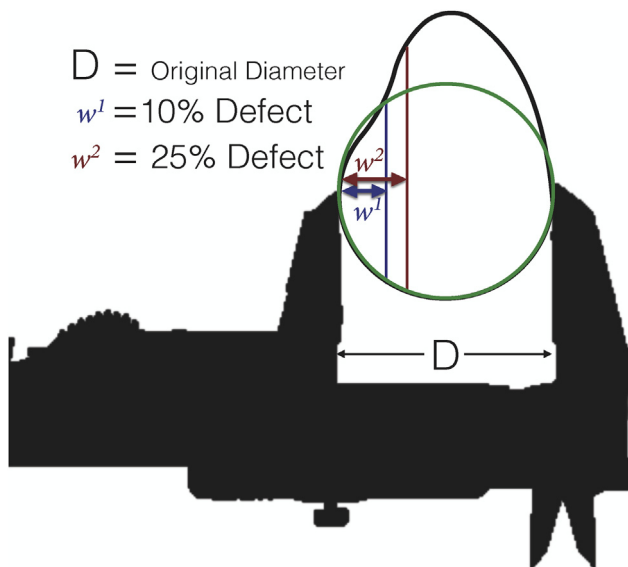


Fig 2. This diagram demonstrates the method used to create the cadaveric defects. The original glenoid maximum diameter (D) was first determined with a digital caliper after soft tissue elevation. Based on this number and the referenced equation, the distance from the posterior glenoid to a vertical line that would create a given defect size based on the circle area calculation was yielded. This included the distance for a 10% ($D-w^1$) and 25% ($D-w^2$) defect size.

Table 1. Average Measured Defect Size Based on Modality

	Measured, %	CT Scan, %	1.5-T MRI, %	3-T MRI, %	ANOVA
0% defect	0 ± 0	0 ± 0	0 ± 0	0 ± 0	
10% defect	11.7 ± 2.4	10.7 ± 1.7	13 ± 2.3	12 ± 2.9	0.27
25% defect	25.6 ± 2.8	23 ± 3.3	22 ± 3.3	24 ± 5.8	0.73
Pearson ρ		0.97	0.93	0.92	

NOTE. Data are presented as mean \pm standard deviation.

ANOVA, analysis of variance; CT, computed tomography; MRI, magnetic resonance imaging; T, tesla.

illustrating the true error in measurements that occur during segmentation or analysis. Consequently, previous studies that have removed all soft tissues tend to report no significant difference in the compared imaging modalities.¹⁷⁻¹⁹ With the labrum and soft tissues intact, the current study also demonstrates that all 3 imaging modalities have similar error in bone loss measurement.

With increasing defect size, the error in bone loss prediction of 3-T MRI, and to a lesser extent 3D CT, increased by 2% to 3%. As described by Huysmans et al.,²³ this study uses a circle to estimate the intact glenoid morphology. As the amount of reference material available is decreased after a template circle is drawn from it, the error in the resulting estimation likely increases. That is to say, the less glenoid one has to reference from, the more likely it is for one's prediction to be inaccurate. This fact is important to keep in mind when reviewing the results of studies such as those by Gytopoulos et al.²⁵ that analyze defects that do not reach this critical threshold. The clinical relevance of this finding is whether these differences in calculated bone loss would alter clinical decision making. The authors speculate that the difference in error with increasing defect size may relate to the accuracy of the imaging modality in an inverse relationship. That is, more data points gives the observer more options for placing the circle. Based on our data, it is possible the increased error in the 1.5-T data for 10% defects, because of relative inaccuracy, minimizes its difference when comparing it to the 25% defect data.

The clinical utility of 3D MRI ultimately relies on its ability to make the same decisions that would be made with other accepted techniques such as 3D CT scans. If one assumes that the clinical cutoff for osseous augmentation procedures is 20%, one can analyze if

Table 2. Correlation Between Different Image Modalities for Measured Defect Size

	CT Scan	1.5-T MRI	3-T MRI
CT scan	1	0.91	0.90
1.5-T MRI		1	0.82
3-T MRI			1

CT, computed tomography; MRI, magnetic resonance imaging; T, tesla.

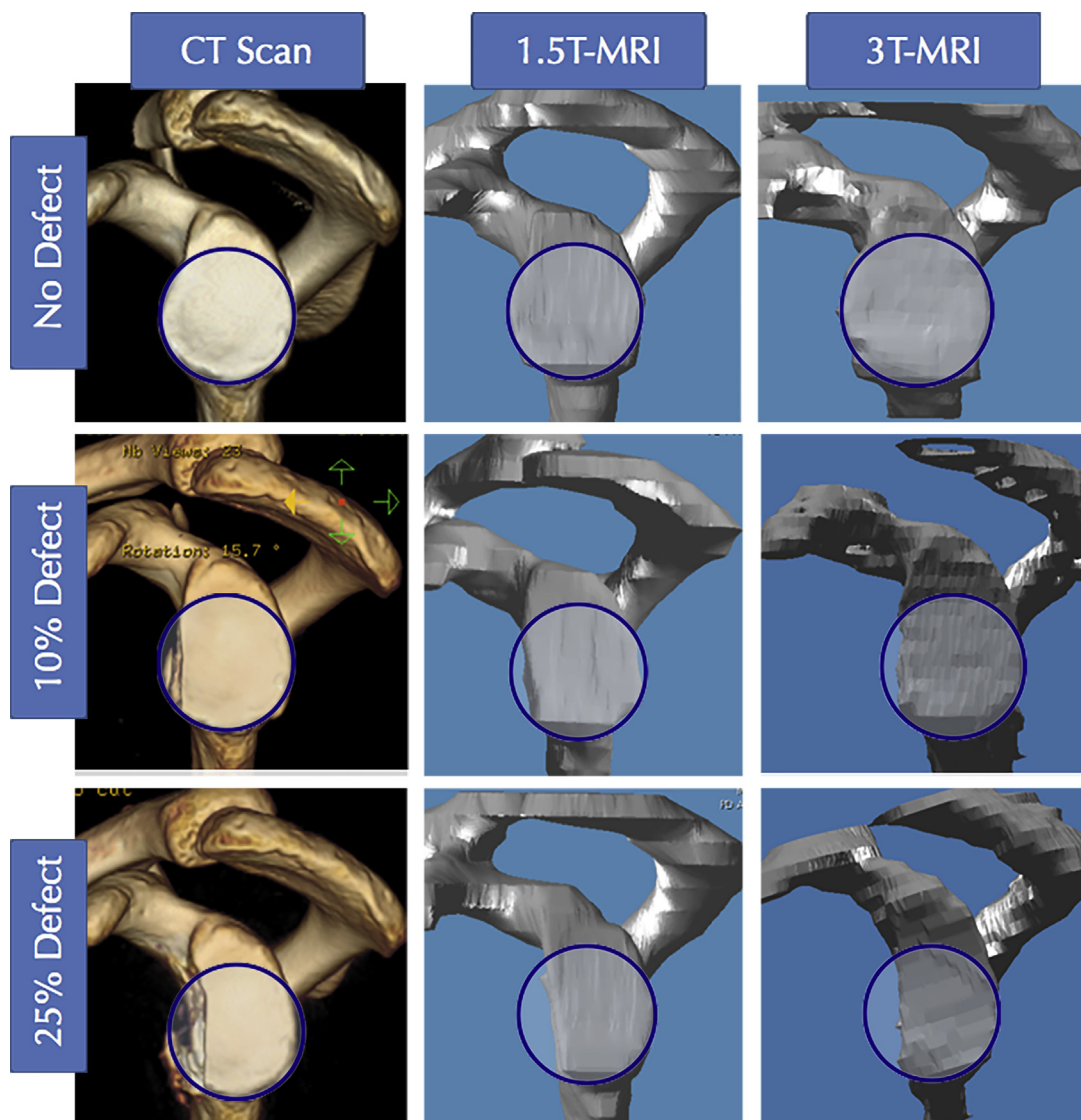


Fig 3. Representative images from a single cadaveric shoulder demonstrating 3-dimensional computed tomography (CT), 1.5-T magnetic resonance imaging (MRI), and 3-T MRI reconstructions. Blue circles estimating the native glenoid have been superimposed.

3D MRI was ever above or below that cutoff when 3D CT scan gave opposing information.^{3,10,26} In this light, all defects smaller than 15% were measured as less than 15% except for one of the 18 (3-T MRI measurement 16.9%). Therefore, all patients who may have been scheduled for a soft tissue procedure based on CT scan would have had the same result based on 3D MRI. With regard to defects larger than 20%, 3 samples were measured as being smaller than 20%. This occurred with multiple modalities, including 1.5-T MRI, 3-T MRI, and CT scan. In one specimen, all 3 modalities (CT, 1.5-T MRI, and 3-T MRI) were below 20% for a defect sized at 26%. In total, of the 36 defect measurements that were performed, 5 may have resulted in a clinically important difference where bone loss was underestimated (2- to 1.5-T MRI, 2- to 3-T MRI, 1-dimensional to 3D CT).

Most important, all studies yield an estimation of the actual amount of bone loss and have inherent error based on both the imaging modality and the measuring technique. However, in 8 of 12 defects, all modalities either over- or underestimated the defect size for a given sample, with the minority of samples having some modalities overestimated whereas others underestimated the size of the same defect. Therefore, factors likely specific to individual shoulder anatomy may increase the likelihood of error based on our assumptions of defect measurement.

Although authors have previously reported methods for 3D reconstructions of the glenoid using MRI, typically they involve complex sequences that require subtraction of secondary sequences to better define the glenoid morphology.²⁵ Radiographs and even 2D advanced imaging modalities, such as MRI or CT, are

Table 3. Absolute Difference Between the Actual and Measured Defect Size

	CT Scan	1.5-T MRI	3-T MRI	ANOVA
10% defect	2.5 ± 1.2	4.0 ± 2.0	3.7 ± 2.1	0.34
25% defect	4.2 ± 2.3	4.9 ± 3.0	6.1 ± 2.7	0.47
<i>t</i> test	0.007	0.51	0.02	

NOTE. Data are presented as mean ± standard deviation.

ANOVA, analysis of variance; CT, computed tomography; MRI, magnetic resonance imaging; T, tesla.

less accurate because of sensitivity to patient positioning and scanning technique. Although 2D MRI is similar to 2D CT in determining bone loss,⁸ cadaveric and clinical studies have shown that both are clearly inferior to 3D CT.^{7,9} Therefore, we have chosen that as the gold standard by which to compare our imaging modalities. All scanning centers already use T1 imaging and this can be easily applied in the clinical setting. The simplicity of our study increases the likelihood of adoption and only adds 3 minutes of MRI scan time per shoulder imaged. Acquiring MRI alone rather than both MRI and CT will decrease the overall cost and time-intensiveness of imaging shoulders and will likely lead to increased implementation of this method. However, currently this method still requires manual segmentation, which will need to be automated to improve reproducibility and increase adoption. Importantly, our study shows that larger magnets (1.5- vs 3-T) may not be necessary to achieve results similar to 3D CT scans.

With regard to the original power analysis, the actual standard deviation for the primary outcome the study was powered for was (in order from lowest to highest)

1.2, 2.0, 2.1, 2.3, 2.7, and 3.0. Based on this (average of 2.21%), the authors believe this was a reasonable assumption.

Limitations

Limitations of the current study include a small sample size with regard to comparisons between defect sizes. Although significant differences were noted when evaluating the difference between actual and measured defect size with 3-T MRI, this was not the primary outcome, and the findings for CT measurements may have been underpowered. Although all attempts were made to create a clinically relevant cadaveric model, the labrum was not reattached back to the glenoid after creating the defect as is often seen clinically, thus making it easier to determine the glenoid edge during the segmentation process. However, it is also worth noting that clinically the labrum often reattaches medially on the glenoid neck, which would still allow clear identification of the glenoid edge. Clinical correlation using this specific methodology is required to determine true clinical utility. Although our group has achieved this and is being used in the lead author's (A.B.Y.'s) clinical practice, the scanning protocol is more involved and may decrease widespread adoption until the automation is similar to that of CT. Additionally, as with other 3D MRI studies,²⁵ the current study relies on manual segmentation to create 3D reconstructions from MRI data; thus, the result may be less reproducible. Automating 3D reconstruction as is common with CT will lead to more reproducible results and improve adoption. As this method was not automated, a weakness of this study is the lack of evaluation of the intra- and interobserver reliability of the

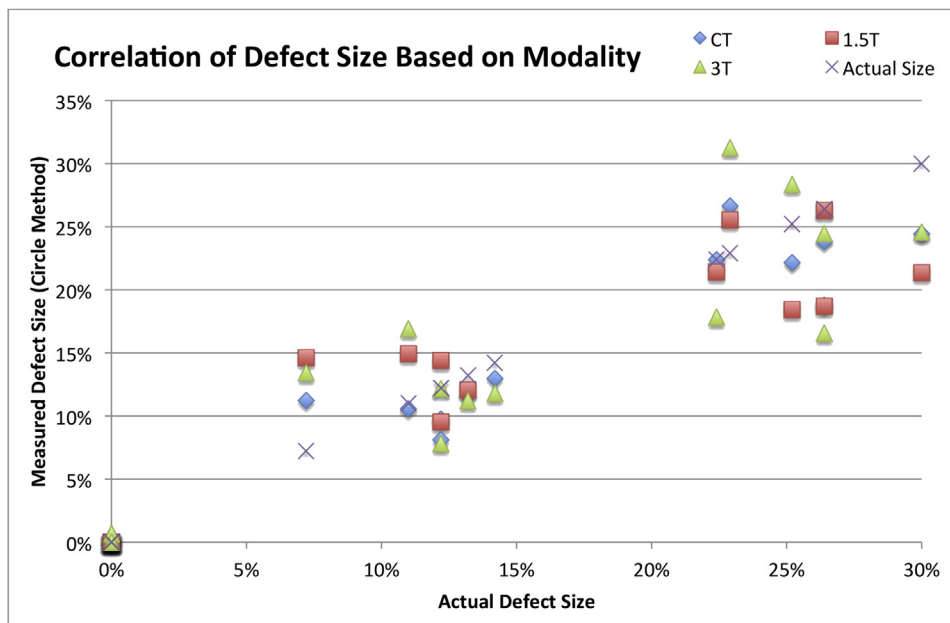


Fig 4. Plot of measured versus actual defect size for all specimens. Of note, one sample in the 10% defect size group had the same defect size as another shoulder. Therefore, these points occur at the same position on the x-axis. (CT, computed tomography; T, tesla.)

segmentation. Moreover, although all attempts were made to obtain the raw axial data in a similar reference plane, differences in this angle could affect the reproducibility of the 3D reconstructions.

Conclusions

Both 1.5- and 3-T–based 3D MRI reconstructions of glenoid bone loss correlate with measurements from 3D CT scan data and actual defect size in a cadaveric model. Regardless of imaging modality, the error in bone loss measurement tends to increase with increased defect size. Use of 3D MRI in the setting of shoulder instability could obviate the need for CT scans.

References

- Kralinger FS, Golser K, Wischatta R, Wambacher M, Sperner G. Predicting recurrence after primary anterior shoulder dislocation. *Am J Sports Med* 2002;30:116-120.
- Rowe CR, Patel D, Southmayd WW. The Bankart procedure: A long-term end-result study. *J Bone Joint Surg Am* 1978;60:1-16.
- Burkhart SS, De Beer JF. Traumatic glenohumeral bone defects and their relationship to failure of arthroscopic Bankart repairs: Significance of the inverted-pear glenoid and the humeral engaging Hill-Sachs lesion. *Arthroscopy* 2000;16:677-694.
- Boileau P, Villalba M, Héry J-Y, Balg F, Ahrens P, Neyton L. Risk factors for recurrence of shoulder instability after arthroscopic Bankart repair. *J Bone Joint Surg Am* 2006;88:1755-1763.
- Tauber M, Resch H, Forstner R, Raffl M, Schauer J. Reasons for failure after surgical repair of anterior shoulder instability. *J Shoulder Elbow Surg* 2004;13:279-285.
- Yamamoto N, Itoi E, Abe H, et al. Effect of an anterior glenoid defect on anterior shoulder stability: A cadaveric study. *Am J Sports Med* 2009;37:949-954.
- Rerko MA, Pan X, Donaldson C, Jones GL, Bishop JY. Comparison of various imaging techniques to quantify glenoid bone loss in shoulder instability. *J Shoulder Elbow Surg* 2013;22:528-534.
- Stecco A, Guenzi E, Cascone T, et al. MRI can assess glenoid bone loss after shoulder luxation: Inter- and intra-individual comparison with CT. *Radiol Med* 2013;118:1335-1343.
- Bishop JY, Jones GL, Rerko MA, Donaldson C, MOON Shoulder Group. 3-D CT is the most reliable imaging modality when quantifying glenoid bone loss. *Clin Orthop Relat Res* 2013;471:1251-1256.
- Chuang T-Y, Adams CR, Burkhart SS. Use of preoperative three-dimensional computed tomography to quantify glenoid bone loss in shoulder instability. *Arthroscopy* 2008;24:376-382.
- Griffith JF, Yung PSH, Antonio GE, Tsang PH, Ahuja AT, Chan KM. CT compared with arthroscopy in quantifying glenoid bone loss. *Am J Roentgenol* 2007;189:1490-1493.
- Biswas D, Bible JE, Bohan M, Simpson AK, Whang PG, Grauer JN. Radiation exposure from musculoskeletal computerized tomographic scans. *J Bone Joint Surg Am* 2009;91:1882-1889.
- Brenner DJ, Hall EJ. Computed tomography—An increasing source of radiation exposure. *N Engl J Med* 2007;357:2277-2284.
- Hayes ML, Collins MS, Morgan JA, Wenger DE, Dahm DL. Efficacy of diagnostic magnetic resonance imaging for articular cartilage lesions of the glenohumeral joint in patients with instability. *Skeletal Radiol* 2010;39:1199-1204.
- Palmer WE, Brown JH, Rosenthal DI. Labral-ligamentous complex of the shoulder: Evaluation with MR arthrography. *Radiology* 1994;190:645-651.
- Dietrich TJ, Zanetti M, Saupe N, Pfirrmann CWA, Fucentese SF, Hodler J. Articular cartilage and labral lesions of the glenohumeral joint: Diagnostic performance of 3D water-excitation true FISP MR arthrography. *Skeletal Radiol* 2010;39:473-480.
- Huijsmans PE, Haen PS, Kidd M, Dhert WJ, van der Hulst VPM, Willems WJ. Quantification of a glenoid defect with three-dimensional computed tomography and magnetic resonance imaging: A cadaveric study. *J Shoulder Elbow Surg* 2007;16:803-809.
- Gyftopoulos S, Yemin A, Mulholland T, et al. 3DMR osseous reconstructions of the shoulder using a gradient-echo based two-point Dixon reconstruction: A feasibility study. *Skeletal Radiol* 2012;42:347-352.
- Gyftopoulos S, Hasan S, Bencardino J, et al. Diagnostic accuracy of MRI in the measurement of glenoid bone loss. *Am J Roentgenol* 2012;199:873-878.
- Bhatia S, Saigal A, Frank RM, et al. Glenoid diameter is an inaccurate method for percent glenoid bone loss quantification: Analysis and techniques for improved accuracy. *Arthroscopy* 2015;31:608-614.e1.
- Saito H, Itoi E, Sugaya H, Minagawa H, Yamamoto N, Tuoheti Y. Location of the glenoid defect in shoulders with recurrent anterior dislocation. *Am J Sports Med* 2005;33:889-893.
- Baudi P, Righi P, Bolognesi D, et al. How to identify and calculate glenoid bone deficit. *Chir Organi Mov* 2005;90:145-152.
- Huysmans PE, Haen PS, Kidd M, Dhert WJ, Willems JW. The shape of the inferior part of the glenoid: A cadaveric study. *J Shoulder Elbow Surg* 2006;15:759-763.
- Sugaya H, Moriishi J, Dohi M, Kon Y, Tsuchiya A. Glenoid rim morphology in recurrent anterior glenohumeral instability. *J Bone Joint Surg Am* 2003;85:878-884.
- Gyftopoulos S, Beltran LS, Yemin A, et al. Use of 3D MR reconstructions in the evaluation of glenoid bone loss: A clinical study. *Skeletal Radiol* 2014;43:213-218.
- Itoi E, Lee SB, Berglund LJ, Berge LL, An KN. The effect of a glenoid defect on anteroinferior stability of the shoulder after Bankart repair: A cadaveric study. *J Bone Joint Surg Am* 2000;82:35-46.